XLVI CILAMCE
VITÓRIA - ES - BRAZIL - 2025
XLVI IBERO-LATIN AMERICAN CONGRESS ON COMPUTATIONAL METHODS IN ENGENEERING

Topology Optimization applied to the Impeller-Diffuser Design of Centrifugal Compressors considering 3D Domains

Camilo A. Plata Uribe[1], Emílio C. Nelli Silva[1]

[1]*Department of Mechatronics and Mechanical Systems Engineering, University of São Paulo*
Av. Prof. Mello Moraes, 2231 - 05508-030, São Paulo, SP, Brazil
camiloplata@usp.br, ecnsilva@usp.br

Abstract. Efficient carbon dioxide compression is crucial to the feasibility of certain carbon capture and storage (CCS) systems, which are indispensable tools in the global effort to mitigate greenhouse gas emissions. Given that compressors are responsible for the majority of energy consumption in some CCS processes, discovering innovative solutions that could enhance the performance of these devices is therefore a relevant engineering challenge. Thus, this study applies topology optimization to the impeller-diffuser configuration in centrifugal compressors, aiming to explore the impact of considering three-dimensional design domains on the resulting topologies and performance metrics under steady state conditions. The optimization problem uses a multi-objective function to minimize energy dissipation while maximizing the impeller pressure head, variation of static pressure in the diffuser, and total energy transfer from the device to the fluid. Accordingly, Results are obtained under laminar and turbulent incompressible steady-state flows in both two-dimensional (2D) and three-dimensional (3D) design domains. Numerical results are included for comparing laminar and turbulent flow regimes, comparing 2D and 3D domain configurations, and varying different weight combinations in the multi-objective function. These results highlight how turbulence modeling and accounting for three-dimensional effects leads to significantly different optimized topologies, offering valuable insights for the design of high-performance centrifugal compressors.

Keywords: Fluid topology optimization, Impeller-diffuser, 3D design domain, Multiple reference frame, Turbulent flow

1 Introduction

The increasing concentration of greenhouse gases has intensified global efforts to reduce emissions. Among various mitigation strategies, Carbon Capture and Storage (CCS) stands out, with centrifugal compressors playing a key role [1]. Enhancing their performance is therefore crucial. One promising approach is fluid flow topology optimization, which strategically distributes fluid and solid within a domain to reveal efficient, often non-intuitive flow paths that meet performance objectives. This work builds on the formulation proposed by Alonso and Silva [2], where the rotor–stator configuration was simplified from a predominantly 2D radial configuration. the Multiple Reference Frame (MRF) or "frozen rotor" approach captures rotational effects by solving the governing equations in a rotating frame within the impeller region, while treating the surrounding flow as stationary. This steady-state model avoids the high cost of transient simulations and enables adjoint-based sensitivity analysis. As stated by Alonso and Silva [2], while the use of a 2D model can be viewed as a first step in the overall design process, it cannot guarantee a fully optimized 3D result. Thus, this work aims to extend and test the MRF formulation in a 3D domain, which considers an axial inlet and radial outlet. Specifically this work focuses on the design of impeller-diffuser configurations in centrifugal compressors. this research seeks to characterize the impact of considering a complete spatial geometry on the optimized topology. This transition allows for the exploration of additional degrees of freedom in the geometry, which significantly expands the search space and favors the emergence of innovative solutions with greater physical fidelity.

The optimization problem uses a multi-objective function to minimize energy dissipation while maximizing impeller pressure head, static pressure difference in the diffuser, and total energy transfer from the device to the fluid. Design variables are defined as a pseudo-density field that controls local porous media resistance, with volume constraints applied to both rotating and stationary zones, the material model is the traditional one presented in Borrvall and Petersson [3], and binary material distribution enforced via the Topology optimization of binary structures (TOBS) algorithm of Sivapuram and Picelli [4]. The fluid flow is governed by the Navier–Stokes equa-

tions with rotational effects modeled using the MRF approach formulated by Alonso and Silva [2], and turbulence is treated with the Wray-Agarwal model in Han et al. [5], a single-equation turbulence model. Sensitivities are computed using a high-level discrete adjoint method combining OpenFOAM and FEniCS/dolfin-adjoint through the FEniCS-TopOpt-Foam library developed by Alonso et al. [6]. Accordingly, Results are obtained under laminar and turbulent incompressible steady-state flows in both 2D and 3D design domains.

2 MRF formulation

This work is based on the formulation of Alonso and Silva [2], that consider a Multiple Reference Frame approach to integrate the fluid flow equations within both stationary (absolute) and rotating (relative) reference frames as shown in Fig. 1a. The continuity and momentum equations that are valid for the whole domain, including the stationary and rotating domains in the frozen rotor approach can be expressed as:

$$\begin{aligned}
&\nabla \cdot \boldsymbol{v}_{\text{abs}} = 0, \text{ and} \\
&\rho \nabla \boldsymbol{v}_{abs} \cdot \boldsymbol{v}_{abs} + f_{\text{MRF}} \left[-\rho \nabla \boldsymbol{v}_{abs} \cdot (\boldsymbol{\omega} \times \boldsymbol{r}) - \rho \nabla (\boldsymbol{\omega} \times \boldsymbol{r}) \cdot (\boldsymbol{v}_{abs} - \boldsymbol{\omega} \times \boldsymbol{r}) \right. \\
&\left. + 2\rho \boldsymbol{\omega} \times (\boldsymbol{v}_{\text{abs}} - \boldsymbol{\omega} \times \boldsymbol{r}) + \rho \boldsymbol{\omega} \times (\boldsymbol{\omega} \times \boldsymbol{r}) \right] = \nabla \cdot \boldsymbol{T} - \kappa(\alpha) \boldsymbol{v}_{\text{mat,rs}},
\end{aligned} \tag{1}$$

where $\boldsymbol{r}$ is the radial coordinate, $\boldsymbol{v}_{\text{abs}}$ is the absolute velocity, $\boldsymbol{\omega}$ is the rotational velocity, and the stress tensor ($\boldsymbol{T}$) is the fluid stress tensor. The terms $2\rho\boldsymbol{\omega} \times (\boldsymbol{v}_{\text{abs}} - \boldsymbol{\omega} \times \boldsymbol{r})$ and $\rho\boldsymbol{\omega} \times (\boldsymbol{\omega} \times \boldsymbol{r})$ are the inertial forces that account for centripetal and coriolis accelerations in the rotating domain. The MRF factor f_{MRF} defines the subdomains: $f_{\text{MRF}} = 1$ in the rotating region Ω_r and $f_{\text{MRF}} = 0$ in the stationary region Ω_s (see Fig. 1a). The additional force term at the right hand side of the momentum equation is used to model the solid material controlled by the inverse permeability $\kappa(\alpha)$ using the continuously varying function proposed by Borrvall and Petersson [3], where α is the design variable for topology optimization (pseudo-density), and The material velocity is defined as $\boldsymbol{v}_{mat,rs} = \boldsymbol{v}_{\text{abs}} - \boldsymbol{\omega} \times \boldsymbol{r}$ in the rotating subdomain Ω_r and $\boldsymbol{v}_{mat,rs} = \boldsymbol{v}_{\text{abs}}$ in the stationary subdomain Ω_s.

2.1 turbulence modeling

When a RANS turbulence model is considered, a statistical time average is taken onto eq. (1) and the stress tensor $\boldsymbol{T}$ is replaced by $(\boldsymbol{T} + \boldsymbol{T}_R)$, where $\boldsymbol{T}_R$ is the Reynolds turbulent stress tensor, which takes into account the turbulent effects (otherwise, for laminar flow, $\boldsymbol{T}_R = 0$). By considering the WA2018 model in Han et al. [5], the MRF formulation applied to the turbulence equations feature scalar variables as follows:

$$\begin{aligned}
&\rho \left[(1 - f_{\text{MRF}}) \boldsymbol{v}_{\text{abs}} + f_{\text{MRF}} (\boldsymbol{v}_{\text{abs}} - \omega \times r) \right] \cdot \nabla R_T = \\
&+ \nabla \cdot \left[(\rho T_R R_T + \mu) \nabla R_T \right] + \rho C_1 R_T S + f_1 C_{1,k-\omega} \rho \frac{R_T}{S} \nabla R_T \cdot \nabla S \\
&- \rho (1 - f_1) \min \left[C_{2,k-\epsilon} R_T^2 \left(\frac{\nabla S \cdot \nabla S}{S^2} \right), C_m \nabla R_T \cdot \nabla R_T \right] - \lambda_{R_T} \kappa(\alpha) R_T,
\end{aligned} \tag{2}$$

where R_T is the undamped turbulent viscosity, λ_{R_T} is the penalization parameter that attenuates turbulence inside the solid material. The rest of the parameters and remaining terms are specified in Han et al. [5]. Note that for simplicity, the state variables were represented with the same notation as in eq. (1), however they represent the statistical time average variables.

2.2 Boundary value problem

The impeller–diffuser configuration boundaries, shown in Fig. 1b, define the boundary value problem for turbulent flow. The computational domain $\Omega = \Omega_r \cup \Omega_s$ includes inlet (Γ_{in}), outlet (Γ_{out}), rotating (Γ_r), stationary (Γ_s), and cyclic (Γ_c) boundaries. At the inlet, velocity and turbulent viscosity are prescribed; on rotating walls, velocity follows rigid-body motion and turbulent viscosity is zero; on stationary walls, a no-slip condition is applied with zero turbulent viscosity. At the outlet, a stress-free condition is used for both velocity and turbulence. Cyclic boundaries enforce periodicity. The Reynolds stress tensor $\boldsymbol{T}_R$ accounts for turbulence, and vanishes in laminar flow.



(a) Rotating and stationary subdomains for the MRF approach

(b) Boundaries with straight blades as initial guess

Figure 1. Schematic of a 2D impeller-diffuser configuration

3 Topology optimization problem formulation

The topology optimization problem that is going to be study can be defined as:

$$
\begin{aligned}
&\underset{\alpha}{\textbf{minimize}}\ J(\boldsymbol{u}(\alpha),\alpha)\\
&\textbf{subjected to}\\
&\quad \text{Fluid volume constraint:}\\
&\quad \text{- Rotating zone: } \int_{\Omega_{\alpha,r}} \alpha\, d\Omega_{\alpha,r} \leq f_r V_{r,0}\\
&\quad \text{- Stationary zone: } \int_{\Omega_{\alpha,s}} \alpha\, d\Omega_{\alpha,s} \leq f_s V_{s,0}\\
&\quad \text{Box constraint: } \alpha : 0 \leq \alpha \leq 1
\end{aligned}
\tag{3}
$$

The topology optimization problem is to minimize the multi-objective function $J(\boldsymbol{u}(\alpha),\alpha)$ (defined in section 3.1), where $\boldsymbol{u}(\alpha) = [p(\alpha), \boldsymbol{v}_{\text{abs}}(\alpha), R_T(\alpha)]$ is the state vector of the simulations for a given α, subjected to volume constraints in both the rotating and stationary zones, and box constraint for the pseudo-density $\alpha : 0 \geq \alpha \geq 1$. f_r and f_s are the specified maximum fluid volume fraction for the rotating and stationary zones, and $V_{r,0} = \int_{\Omega_{\alpha,r}} d\Omega_{\alpha,r}$ and $V_{s,0} = \int_{\Omega_{\alpha,s}} d\Omega_{\alpha,s}$ are the volumes of rotating and stationary zones of the design domains ($\Omega_{\alpha,r}$ and $\Omega_{\alpha,s}$, respectively).

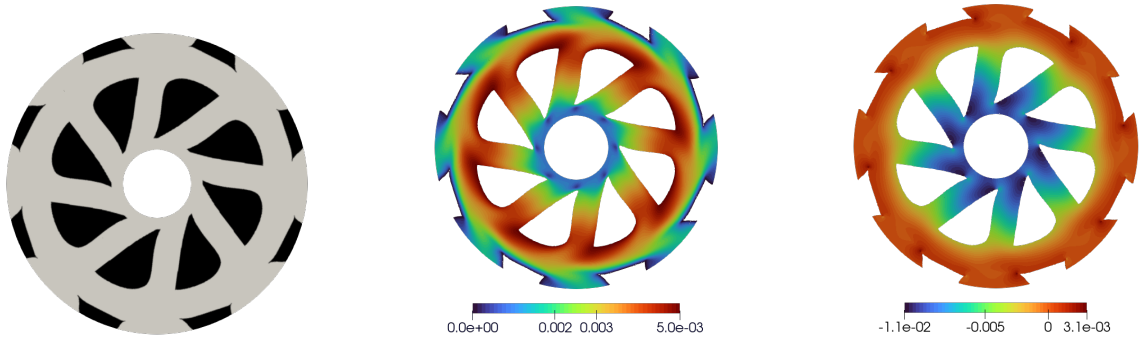
3.1 Multi-objective function

Four objectives are taken into account to optimize the impeller-diffuser configuration. The first objective is to minimize the zone-relative energy dissipation Borrvall and Petersson [3], but also considers the inertial effects presented in Alonso et al. [7] only inside the rotating zone. The second objective is to give more importance to the maximization of the performance of the rotor; particularly, to increase the pressure head inside the rotor. The third objective is to increase the static pressure energy gained inside the diffuser. Since the first and second objectives are relative measures (related to performance/dissipation), and the third objective is an absolute measure, it is possible for the third objective to pull the overall energy transfer down while still improving the performance. Therefore, the fourth objective is to increase the overall energy transferred from the whole device to the fluid. This is done through the (absolute) pressure head, This functions are explicitly set in the multi-objective function by dividing each objective function by its corresponding value in the initial guess, and then scaling by the initial value of one of the objective functions.

4 Results

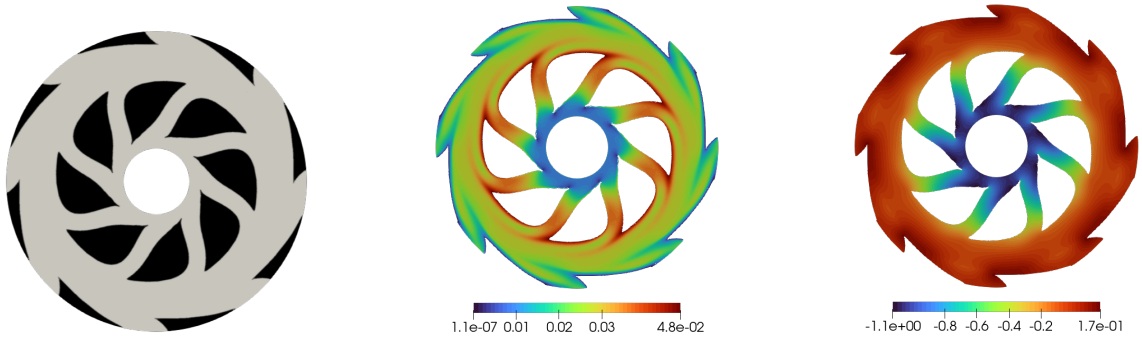
Some numerical results for a 2D configuration under laminar and turbulent incompressible flow are presented in Fig. 2 and Fig. 3, respectively. Both solutions exhibit a characteristic division between the rotor region and diffuser region, with smooth transitions and clear rotational symmetry.

The pseudo-density fields (Fig. 2a and Fig. 3a) highlight a notable geometric difference: in the turbulent case, the rotor blades are more tilted and curved, resembling traditional backward-swept impeller blades. Conversely, the laminar configuration favors more radial and straighter blades, adequate for lower Reynolds number flows. Similarly, the diffuser (stator) region shows design differences. In the laminar topology, the diffuser vanes are broader and more closely spaced. In the turbulent regime, the stator blades are more aerodynamically contoured, with increased spacing.



(a) pseudo-density, α (b) Absolute velocity, $\boldsymbol{v}_{\text{abs}}$ [m/s] (c) Pressure, p [Pa]

Figure 2. Simulations of a 2D laminar optimized topology ($W_{\Phi} = 8$, $W_{H,r} = 1$, $W_{p,s} = 0.05$ and $W_{H,rs} = 0.5$).



(a) pseudo-density, α (b) Absolute velocity, $\boldsymbol{v}_{\text{abs}}$ [m/s] (c) Pressure, p [Pa]

Figure 3. Simulations of a 2D turbulent optimized topology ($W_{\Phi} = 8$, $W_{H,r} = 1$, $W_{p,s} = 0.05$ and $W_{H,rs} = 0.5$)

This type of result will be used as a comparative reference for analyzing the effects of three-dimensionality on the performance of the optimized topologies, initially addressing incompressible fluid flow in laminar and turbulent regime. Fig. 4 presents the 3D design domain setup considered for the optimization tests currently underway. This geometry contains the rotating and stationary regions, as well as the cyclic interfaces and the inlet and outlet boundaries, suitable for the application of the MRF formulation. The expectation is that the inclusion of three-dimensionality will reveal complex flow behaviors, such as three-dimensional vorticity patterns, localized recirculation, and general variations in momentum transport in the domain, which are not fully captured in two-dimensional simulations, with the potential for additional gains in the device efficiency.

5 Conclusions

Preliminary tests validate the functionality of the framework across multiple configurations. Ongoing work includes a systematic comparison between laminar and turbulent regimes, 2D and 3D configurations, and the impact of different weighting schemes in the multi-objective function. These analyses aim to further validate the flexibility of the framework and quantify trade-offs between energy dissipation, pressure head gain, and pressure recovery. The preliminary application of the studied topology optimization framework confirms its effectiveness in generating optimized structures across various flow regimes and domain configurations. The results highlight how

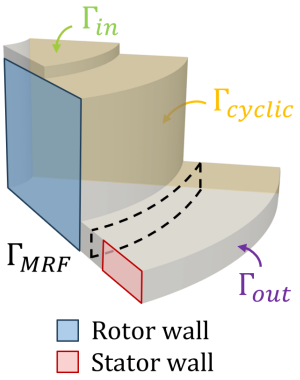


Figure 4. Schematic of the 3D design domain

turbulence modeling and accounting for 3D effects leads to significantly different optimized topologies, offering valuable insights for the design of impeller-diffuser configuration in centrifugal compressors.

Acknowledgements. This research was partly supported by CNPq (Brazilian National Research Council) and FUSP (University of São Paulo Foundation). The authors thank the supporting institutions. The authors also gratefully acknowledge support of the RCGI - Research Centre for Greenhouse Gas Innovation, hosted by the University of São Paulo (USP) and sponsored by FAPESP - São Paulo Research Foundation (grant 2014/50279-4 and 2020/15230-5) and Shell Brasil, and the strategic importance of the support given by ANP (Brazil's National Oil, Natural Gas and Biofuels Agency) through the R&D levy regulation.

Authorship statement. The authors hereby confirm that they are the sole liable persons responsible for the authorship of this work, and that all material that has been herein included as part of the present paper is either the property (and authorship) of the authors, or has the permission of the owners to be included here.

References

[1] International Energy Agency. Net zero by 2050: A roadmap for the global energy sector, 2021.
[2] D. H. Alonso and E. C. N. Silva. Topology optimization for fluid flow devices modeled through the multiple reference frame approach. *Applied Mathematical Modelling*, vol. 118, 2023.
[3] T. Borrvall and J. Petersson. Topology optimization of fluids in stokes flow. *International Journal for Numerical Methods in Fluids*, vol. 41, 2003.
[4] R. Sivapuram and R. Picelli. Topology optimization of binary structures using integer linear programming. *Finite Elements in Analysis and Design*, vol. 139, 2018.
[5] X. Han, M. M. Rahman, and R. K. Agarwal. Development and application of a wall distance free wray-agarwal turbulence model (wa2018). In *AIAA Aerospace Sciences Meeting, 2018*, 2018.
[6] D. H. Alonso, L. F. G. Rodriguez, and E. C. N. Silva. Flexible framework for fluid topology optimization with openfoam® and finite element-based high-level discrete adjoint method (fenics/dolfin-adjoint). *Structural and Multidisciplinary Optimization*, vol. 64, 2021.
[7] D. H. Alonso, de L. F. N. Sá, J. S. R. Saenz, and E. C. N. Silva. Topology optimization based on a two-dimensional swirl flow model of tesla-type pump devices. *Computers and Mathematics with Applications*, vol. 77, 2019.